



Effect of Chloride Ions on Electrodeposition of CdTe from Ammoniacal Basic Electrolytes

Kentaro Arai, Kuniaki Murase,* Tetsuji Hirato,* and Yasuhiro Awakura^z

Department of Materials Science and Engineering, Kyoto University, Yoshida-hommachi, Sakyo-ku, Kyoto 606-8501, Japan

Electrodeposition of CdTe was carried out using ammoniacal basic electrolytes containing chloride ions in order to investigate the effect of chloride ions on the electrodeposition behavior and on the properties of the resulting CdTe deposits. Photoeffect on CdTe electrodeposition, that is, the increase in the deposition rate under irradiation of white visible light onto the growing surface of the CdTe, was depressed with increasing concentration of chloride ions in the deposition bath, while all the irradiation conditions gave flat, smooth, and polycrystalline CdTe layers with almost stoichiometric composition (49.1–51.7 atom % Cd). Both the Cd content and crystallinity of the resulting deposits increased with increasing concentration of chloride ions in the electrolytes. The as-deposited CdTe layer prepared from the chloride electrolyte had an n-type conduction, although the CdTe layer obtained from the sulfate electrolyte was p-type, suggesting that chloride ions in the electrolyte became incorporated into the CdTe layer and formed the donor level.

© 2006 The Electrochemical Society. [DOI: 10.1149/1.2150159] All rights reserved.

Manuscript submitted June 30, 2005; revised manuscript received October 22, 2005. Available electronically January 6, 2006.

CdTe is a promising material for solar cell applications^{1–5} because its bandgap of 1.45 eV at room temperature is suitable for energy conversion from sunlight to electricity. Since CdTe has a high optical-absorption coefficient, a CdTe layer with thickness of 1–2 μm is enough for thorough absorption of sunlight. In addition to some dry or nonwet processes such as screen printing and close-spaced sublimation, electrodeposition^{6–8} has been investigated for the preparation of thin-layered compound semiconductors for solar cell applications, and the cell made up of an n-CdS/p-CdTe heterojunction has been put into production on an industrial scale.⁹ Since the pioneering work of Kröger's group in the late 1970s,⁶ aqueous acidic sulfate electrolytes have historically and almost exclusively been employed as the bath for CdTe electrodeposition,¹⁰ although organic electrolytes¹¹ have also been studied. In contrast, we have proposed that aqueous basic, or alkaline, electrolytes containing ammonia are also suitable for the electrodeposition of a uniform CdTe layer, since these basic solutions have a relatively high solubility of Te(IV) species as TeO_3^{2-} ions.^{12–17} From the basic electrolytes, we successfully obtained smooth and flat polycrystalline CdTe deposits with a nearly stoichiometric composition at potentials positive to that of bulk-Cd deposition.¹⁴ Furthermore, it turned out that the deposition rate was considerably increased by photoirradiation of the cathode surface during the electrodeposition.¹⁸

In both acidic and basic media, CdTe has been electrodeposited mainly from electrolytes containing sulfate ions (SO_4^{2-}) as counter anions of Cd(II) ions. Although in acidic^{19–23} media, electrodeposition of CdTe from some electrolytes with an additional concentration of chloride ions or from CdCl_2 electrolytes has been reported, there are few reports in basic media.^{24,25} The addition of chloride ions into the plating solution yielded a CdTe layer with a better performance of solar cells,¹⁹ although the effect of chlorine on the film characteristics has not been discussed explicitly in any of these publications. In addition, it has been briefly reported that the crystallinity of CdTe increases slightly when replacing sulfate ions in the electrolyte with chloride ions in the basic media.²⁵ A specific adsorption of counteranions on the surface of electrodes can affect the electrodeposition behavior and the properties of deposited CdTe through inclusion of the anions into the deposits. In this study, we report the electrodeposition behavior and the structural and electrical properties of CdTe films deposited from the ammoniacal basic electrolyte containing chloride ions as counteranions.

Experimental

Three ammoniacal basic electrolytes (Table I) with different anions were used for CdTe electrodeposition. The first solution, termed “sulfate electrolyte,” was prepared by dissolving 40 mM $\text{CdSO}_4 \cdot 8/3\text{H}_2\text{O}$ and 10 mM TeO_2 in an ammoniacal buffer solution containing 4.0 M $\text{NH}_3(\text{aq})$ and 0.5 M $(\text{NH}_4)_2\text{SO}_4$.²⁶ The second one, i.e., “chloride electrolyte,” was prepared as for the sulfate electrolyte but dissolving 40 mM $\text{CdCl}_2 \cdot 5/2\text{H}_2\text{O}$ and 1.0 M NH_4Cl instead of 40 mM $\text{CdSO}_4 \cdot 8/3\text{H}_2\text{O}$ and 0.5 M $(\text{NH}_4)_2\text{SO}_4$. The third solution was an equivolume mixture of the sulfate and chloride electrolytes, containing 270 mM of sulfate ions and 540 mM of chloride ions as counteranions. Only counteranions were different for the three electrolytes, while the concentrations of Cd(II) and Te(IV) ions and total ammonia (sum of ammonia and ammonium ions) were unified for all electrolytes; the concentration of Cd(II) ions, Te(IV) ions, and total ammonia were 40 mM, 10 mM, and 5.0 M, respectively. All chemicals (Nacalai Tesque, Inc.) were of reagent grade and were used without pretreatment. The deionized water used to prepare the ammoniacal buffer had a specific resistance larger than $5 \times 10^6 \Omega \text{ cm}$. The pH values of the sulfate, chloride, and mixed electrolytes were 10.7, 10.2, and 10.3 at 298 K (25°C), respectively.

Electrochemical experiments were carried out using a conventional three-electrode setup. Cathodic polarization curves were obtained by scanning the potential of a working electrode with an electrochemical analyzer (ALS 660-A) at the constant scan rate of 10 mV s^{-1} . Cathodic electrodeposition was performed under potentiostatic conditions at the potential -0.4 to -0.7 V using a potentiostat (Hokuto Denko HA-151) connected to a coulometer (Hokuto Denko HF-201). A gold-plated copper sheet ($15 \times 30 \text{ mm}$) and platinum sheet ($20 \times 25 \text{ mm}$) were employed as the working and counter electrodes, respectively, for all experimental runs. The Au/Cu sheet was polished with $0.3\text{-}\mu\text{m}$ alumina abrasive before being used for the cathode substrate; the thickness of the Au plating was $1\text{--}3 \mu\text{m}$. A part of the Au/Cu sheet surface was covered with Teflon adhesive tape so that a set of two squared areas (about $10 \times 10 \text{ mm}^2$) was exposed to the electrolytes as the surface of the substrate. The deposit on one square was transferred onto an epoxy resin²⁵ to examine the electrical properties and that on the other was used for characterization of the crystallinity, composition, and thickness. An Ag/AgCl electrode (Horiba 2080A-06T) immersed in 3.33 M KCl was used as a reference to measure the cathode potential; the potentials were recalculated for the standard hydrogen electrode (SHE). The electrolyte was thermostatted at 343 K (70°C) and stirred at approximately 500 rpm. These electrochemical experiments were performed under white light irradiation or in the dark. A 500-W xenon arc lamp (Wacom KXL-500F) installed in a lamp housing was used for the irradiation. The approximate integrated

* Electrochemical Society Active Member.

^z E-mail: yasuhiro.awakura@materials.mbox.media.kyoto-u.ac.jp

Table I. Composition of electrolytes used for CdTe electro-deposition.

	Sulfate electrolyte	Chloride electrolyte	Mixed electrolyte
CdSO ₄	40 mM		20 mM
CdCl ₂		40 mM	20 mM
TeO ₂	10 mM	10 mM	10 mM
(NH ₄) ₂ SO ₄	0.5 M		0.25 M
NH ₄ Cl		1.0 M	0.5 M
NH ₃ (aq)	4.0 M	4.0 M	4.0 M
pH	10.7	10.2	10.3

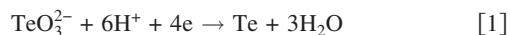
irradiance of the white light just before the electrolytic vessel was 300 mW cm⁻². When deposited in the dark, the electrolytic cell was placed in a light-resistant box to eliminate any photoeffects²⁷ on the growing CdTe.

The compositions of the deposits were determined by electron probe microanalysis. A single crystal of CdTe which is exactly stoichiometric in composition was used as the standard for the analysis. The thickness of deposits was evaluated by surface texture measurements (Tokyo Seimitsu 1400D-12M). In order to confirm the existence of chlorine in the deposits, fluorescent X-ray spectroscopy (Shimadzu XRF-1700) was employed with the fundamental parameter (FP) method. This method is a semiquantitative way to calculate the contents of elements from a set of fluorescent X-ray intensities based on the principle of fluorescent X-ray generation. The morphology and crystallinity of the resulting deposits were examined with an X-ray diffractometer (Rigaku RINT 2200) fitted with a molybdenum X-ray tube. All the X-ray diffraction (XRD) measurements were carried out with the scan mode of 2θ-θ. The reflective spectra of deposits were measured by a spectrophotometer (Hitachi U-3500) with an integrating sphere, in order to determine the band-gap energy.

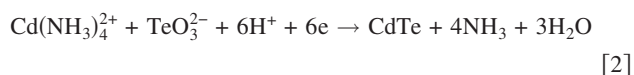
The electrical properties such as resistivity, conduction type, and Hall voltage were measured at room temperature with a resistivity/Hall measurement system (Toyo Corp. ResiTest 8310) using the van der Pauw method.²⁸ Hall measurement was employed in the ac magnetic field method; the magnitude and frequency of the magnetic field were 0.6 T at the maximum and 50 mHz, respectively. The carrier density and mobility were calculated based on these electrical properties. It is difficult to measure the electrical properties of CdTe on the conductive Au/Cu substrate, so the CdTe layer was transferred from the substrate onto nonconductive epoxy resin (Torr Seal; Varian Associates).²⁶ The detailed preparation method for measuring electrical properties is described in a previous paper.²⁹

Results and Discussion

Deposition behavior of CdTe.— Figure 1 shows the cathodic polarization curves for the sulfate, chloride, and mixed electrolytes containing 40 mM Cd(II) and 10 mM Te(IV) in the illuminated and dark conditions. According to a study by Murase et al.,¹⁶ the cathodic current at potentials positive to -0.3 V in the polarization curves for the sulfate electrolyte is attributed to the deposition of elemental Te



while the current at the potentials negative to -0.3 V is attributed to that of CdTe



When assessed from potential-pH diagram of the Te-H₂O system, further reduction of elemental Te to Te²⁻ or Te₂²⁻ ions cannot occur in the potential range from -0.3 to -0.7 V. As observed with the sulfate electrolyte (Fig. 1a), the chloride and mixed electrolytes gave a cathode current at similar potentials negative to -0.3 V, indicating

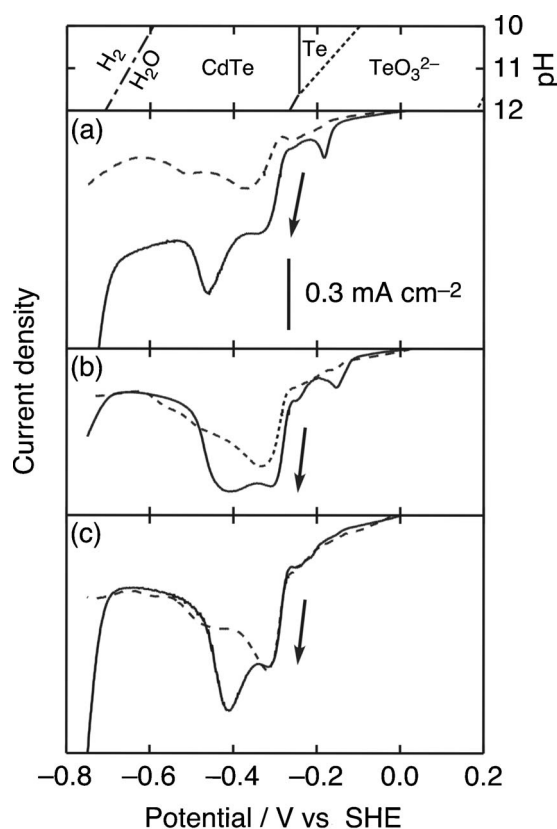


Figure 1. Cathodic polarization curves for the (a) sulfate, (b) chloride, and (c) mixed electrolytes (Table I) containing 40 mM Cd(II) and 10 mM Te(IV) at 343 K. Solid and dashed lines represent illuminated and dark conditions, respectively. Arrows indicate the sweep direction of cathodic potential. Au-plated Cu substrate was used for the working electrode. Sweep rate 10 mV s⁻¹.

that these two electrolytes can also electrodeposit CdTe. In all electrolytes, a second cathodic current peaked at around -0.4 V was recognized under illumination, while the current peak was not clearly observed in the dark condition. The profile of the second peak is dependent on the electrolyte used. In the electrolytes containing chloride ions (chloride and mixed electrolytes), the peak slightly shifted positively compared with the case of the sulfate electrolyte. Furthermore, the peak became weak with increasing chloride ions in the electrolytes. This difference may be related to a slight difference in the composition of deposits specific to illuminated chloride and mixed electrolytes as described later. The rise of cathodic current at about -0.73 V was observed only under illumination in all electrolytes. It is expected that the increase of the current is caused by the deposition of elemental Cd, because the Cd deposition occurs at -0.732 V thermodynamically. In these cases, however, the anodic current peak attributable to the dissolution of elemental Cd could not be seen in the subsequent anodic sweep (not shown in Fig. 1).¹⁶ Hence, it can be considered that the rise in current density is caused not by elemental Cd but by CdTe deposition. The deposition current of CdTe in the sulfate electrolyte was increased by the irradiation of white light as previously reported.¹⁸ In the chloride and mixed electrolytes, however, the cathodic currents under illumination were almost the same as those in the dark. This suggested that photoassisted electrodeposition of the CdTe layer may not occur in the presence of chloride ions in the electrolyte.

Figure 2 depicts the variation of current density during the CdTe deposition at potential -0.7 V under illumination or in the dark. In dark conditions, all the electrolytes followed almost the same trend

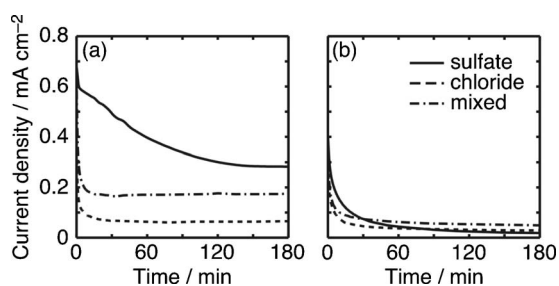


Figure 2. Variations of current densities during CdTe electrodeposition in the potentiostatic condition of -0.7 V from three different electrolytes containing 40 mM Cd(II) and 10 mM Te(IV) (a) under illumination or (b) in the dark.

in the variations of current density; the initial current was about $400 \mu\text{A cm}^{-2}$ but decreased to $<100 \mu\text{A cm}^{-2}$ with time. In contrast, current density under illuminated conditions showed different behaviors depending on the electrolytes employed: In the case of sulfate electrolytes, the current started at $700 \mu\text{A cm}^{-2}$ and decreased with time, but was still larger than $300 \mu\text{A cm}^{-2}$ after 2 h deposition. In the mixed and chloride electrolytes, the currents steeply dropped to less than 200 and $100 \mu\text{A cm}^{-2}$, respectively, within 30 min after starting each deposition. In other words, photo-assisted growth of CdTe¹⁸ was depressed with increasing concentration of chloride ions in the electrolyte. The current for the chloride electrolyte observed under illumination was almost the same level as that in the dark. As described later, the electrical properties of the CdTe layer from the chloride electrolyte are different from those from the sulfate electrolyte. Hence, it was presumed that the depression of the photoeffect is attributable to the difference in the properties of CdTe film. In order to clarify this issue, an additional experiment was performed. CdTe was electrodeposited on the Au/Cu substrate at potential -0.7 V from the chloride electrolyte at the total charge of 0.4 C cm^{-2} under illumination. The resulting CdTe layer was then rinsed for 60 s with deionized water at 343 K and transferred into the sulfate electrolyte to conduct additional electrodeposition of CdTe on it at -0.7 V (Fig. 3). Despite the presence of the underlying CdTe layer prepared from the chloride electrolyte, the photoeffect was not depressed in the sulfate electrolyte. This

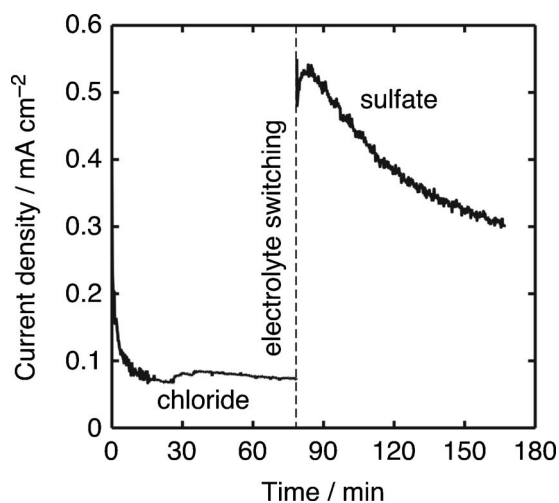


Figure 3. Variation of current density during CdTe electrodeposition under illumination at potential -0.7 V from the chloride electrolyte followed by the sulfate electrolyte. After deposition from the chloride electrolyte for 80 min, resulting CdTe was rinsed with deionized water at 343 K and transferred into the sulfate electrolyte for another deposition for 90 min. The total charge of CdTe electrodeposition in the chloride electrolyte was 0.4 C cm^{-2} .

Table II. Composition of layers (atom % Cd) electrodeposited in potentiostatic conditions of -0.7 to -0.4 V from three different electrolytes listed in Table I. Thickness of the layers was approximately $1.0 \mu\text{m}$.

Cathode potential (V vs SHE)	Sulfate electrolyte	Chloride electrolyte	Mixed electrolyte
-0.7	49.6	51.7	49.8
-0.6	49.8	50.8	50.7
-0.5	49.5	49.7	49.9
-0.4	49.1	49.9	49.5

clearly demonstrated that the depression of the photoeffect of CdTe growth is not caused by the electrical properties of growing CdTe film but by another factor(s) outside the CdTe layer, such as chloride-ion adsorption on the growing surface or modification of metal ions in the electrolyte.

Composition and morphology of the deposits.—Composition of the layers electrodeposited from the three different electrolytes at -0.7 , -0.6 , -0.5 , and -0.4 V potentials under illumination is summarized in Table II. Thickness of the layers was approximately $1.0 \mu\text{m}$. For all the electrolytes, there was a tendency for the Cd content of the CdTe layers to slightly increase with decreasing cathode potential. According to thermodynamic consideration, CdTe compound can electrodeposit at potentials more negative to -0.216 V at pH 10.7, while the deposition potential of elemental Cd is -0.732 V. The change in Cd content is due to the change in overpotential for the reduction of Cd(II) ions to form CdTe. It was found that in addition to the deposition potential, the concentration of chloride ions in the electrolyte also affects the composition of CdTe; the Cd content increased slightly with the chloride ion concentration. Such an increase in Cd content corresponds to a relative depression of the deposition of Te atoms. Because the potentials for CdTe deposition are positive to elemental Cd deposition, Cd atoms cannot deposit unless Te atoms exist at the growing surface. Thus, the growth of CdTe is limited by the preceding deposition of Te atoms. From this point of view, the depression of CdTe growth under illumination and the change in composition may well be attributed to the inhibition of the reduction of Te(IV) in the presence of chloride ions. A specific adsorption of chloride ions may reduce the effective area of the cathode surface and/or delay the electron transfer from cathode to Te(IV) ions. The detection of chlorine from the resulting CdTe layer (see below) is collateral evidence of the adsorption of chloride ions, which causes nonfaradaic inclusion of chlorine.

Figure 4 illustrates XRD patterns of deposits electrodeposited at the potential of -0.7 V from the three different electrolytes. Each diffraction peak could be assigned to CdTe or Au/Cu substrate except the film from the chloride electrolyte under illumination; in this case the pattern included a small reflection attributed to elemental Cd at $2\theta = 14.5^\circ$.³⁰ This indicates that the deposit prepared from the chloride electrolyte under illumination contains a small amount of elemental Cd together with polycrystalline CdTe, although the deposition potential, i.e., -0.7 V, is positive to the Nernst potential of elemental Cd deposition from Cd^{2+} -ammonia complex(es). Some kind of mixed-ligand complex of Cd(II) formed in the presence of chloride ions may be involved in the positive shift of the Cd deposition potential compared to -0.732 V. However, it seems that, at pH 10–11, ammine complexes of Cd(II) ions are more stable than chloride complexes. Hence, the deposition of elemental Cd under illumination could be related to a photoinduced underpotential deposition. Similar phenomena were observed in our previous study using sulfate bath.¹⁸ Regarding the CdTe 111 reflection, the peak for the chloride electrolyte was the strongest among three electrolytes both under illumination and in the dark, although they have the same thickness. According to the mean crystallite sizes of the CdTe deposits (Table III) estimated from the half-width of the 111 peak

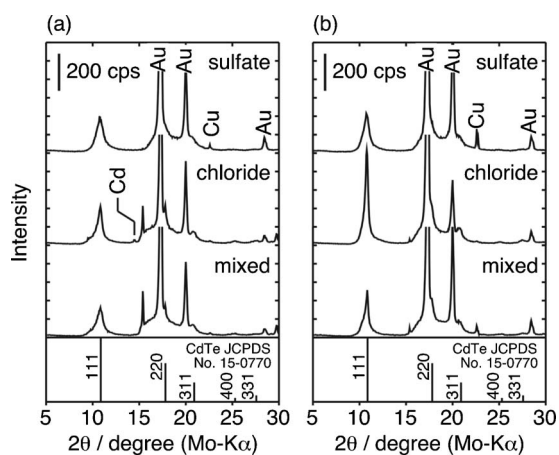


Figure 4. XRD patterns of deposits electrodeposited at potential -0.7 V from three different electrolytes (a) under illumination and (b) in the dark. Thickness of the deposits was about $1\text{ }\mu\text{m}$.

using Scherer's equation, the crystallinity of CdTe became high with increasing concentration of chloride ions in the electrolyte. For all the electrolytes, the mean crystallite size of deposits obtained in the dark was larger than that under illumination, as already reported for a number of sulfate electrolytes.³¹ Given that chloride ions are adsorbed on the growing surface, the number of effective nucleation sites is cut down, yielding a larger crystallite size of CdTe.

Figure 5 shows surface scanning electron microscopy (SEM) images of CdTe layers electrodeposited at potential -0.7 V from the three different electrolytes under illumination and in the dark. Although the surface of the CdTe layer from the sulfate electrolyte was rather flat and smooth, granular deposits with a diameter of $1\text{--}5\text{ }\mu\text{m}$ were recognized on the surface of the CdTe layers from the chloride and mixed electrolytes under illumination; this granular structure is probably due to the inherent nature of elemental Cd, which is apt to electrodeposit dendritically. When assessed from the granular morphology of the surface, the content of elemental Cd in the deposit increased with the concentration of chloride ions in the electrolyte, as detected by XRD measurement. Codeposition of elemental Cd in a previous study¹⁸ also gave a similar surface texture. In contrast, some dendritic deposits with diameters of $5\text{--}10\text{ }\mu\text{m}$ were observed on the surface of the CdTe from both the sulfate and mixed electrolytes in the dark condition. According to the overall composition of the layer, these dendritic deposits may be attributable to elemental Te, although no peaks for elemental Te were observed in the XRD patterns because the amount of the elemental Te is extremely small. The surface of the CdTe layer from the chloride electrolyte in the dark was flat and smooth like that from the sulfate electrolyte under illumination.

CdTe layers electrodeposited from the three different electrolytes were analyzed by fluorescent X-ray spectroscopy in order to examine the presence of chlorine in the CdTe deposits (Fig. 6). Here, the semiquantitative FP method was used to identify the chlorine in the deposits without standard samples. The deposits from the electrolytes containing the chloride ions gave a Cl K α peak at photon energy of about 2620 eV , suggesting the inclusion of chlorine atoms

Table III. Mean crystallite sizes (nm) of CdTe layers electrodeposited at potential -0.7 V from three different electrolytes listed in Table I.

Condition	Sulfate electrolyte	Chloride electrolyte	Mixed electrolyte
Under illumination	6.3	9.7	8.3
In the dark	7.0	15	15

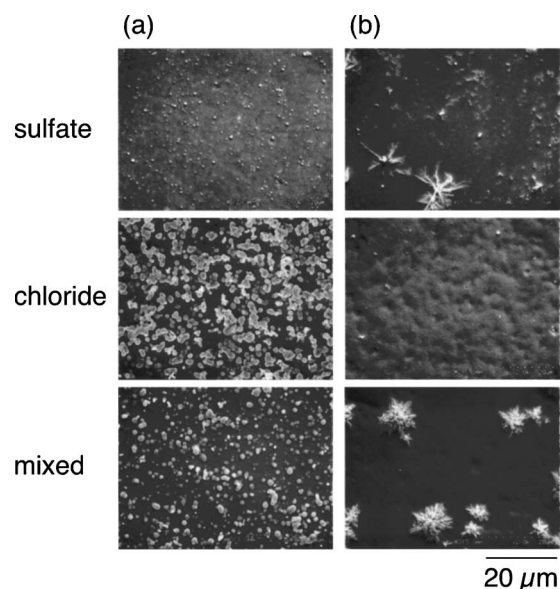


Figure 5. Surface SEM images of CdTe electrodeposited at potential -0.7 V from the three different electrolytes (a) under illumination and (b) in the dark. The thickness of the deposits was $1\text{ }\mu\text{m}$.

in the CdTe layer. It was confirmed from each of the spectral intensities that the chlorine contents in the CdTe deposits increased with the increase of chloride ions in the electrolyte.

Evaluation on the bandgap energy.—Figure 7 depicts the reflectivity spectra of CdTe electrodeposited at potential -0.7 V from the sulfate and chloride electrolytes compared with that of the single-crystal CdTe. The thickness of each CdTe layer was approximately $5\text{ }\mu\text{m}$. The single-crystal CdTe was a plate with thickness of 1 mm . In all spectra, a decrease in reflectivity was observed at al-

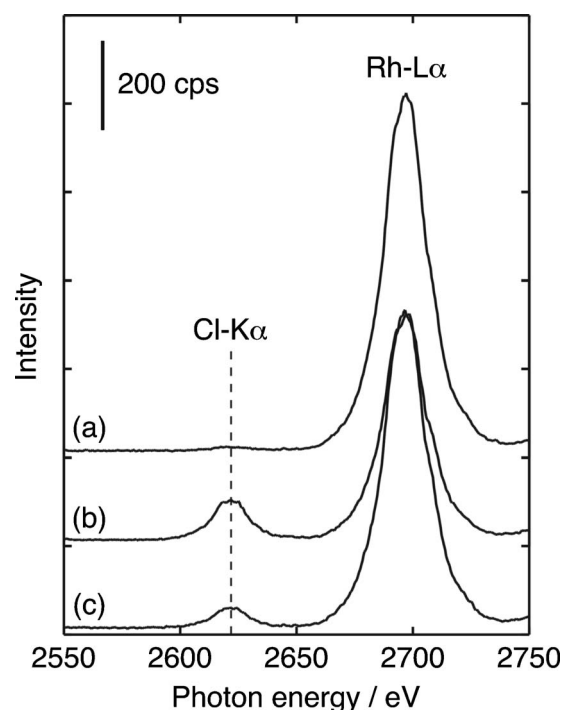


Figure 6. Fluorescent X-ray spectra of CdTe layers electrodeposited at potential -0.7 V from the (a) sulfate, (b) chloride, and (c) mixed electrolytes under illumination.

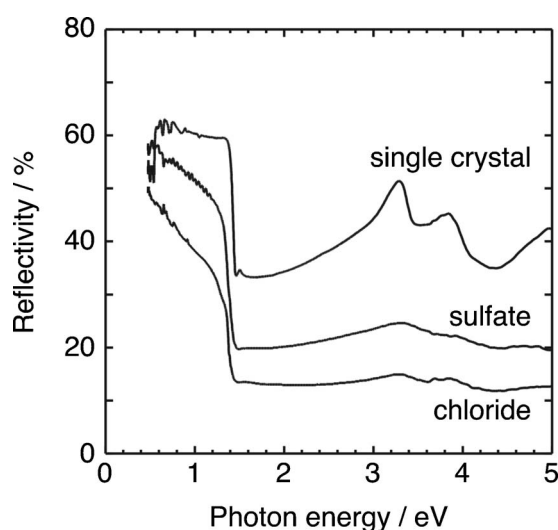


Figure 7. Reflectivity spectra of CdTe layers (thickness 5 μm) electrodeposited at potential -0.7 V from the sulfate and chloride electrolytes under illumination. The spectrum for the single-crystal CdTe plate (thickness 1 mm) is also indicated.

most the same energy corresponding to the bandgap. The bandgap energy of CdTe obtained from the chloride electrolyte was estimated to be 1.45 eV, i.e., the same as that of both CdTe from the sulfate electrolyte and single-crystal CdTe. However, the reflectivity started to decrease from the energy below 1 eV in the electrodeposited CdTe, whereas the decrease in the reflectivity was steep in the single-crystal CdTe. In other words, the absorptions at the edge of bandgap energy of both CdTe from the sulfate and chloride electrolytes were less clear than that of the single-crystal CdTe. This indicates that the CdTe from the chloride electrolyte has some localized impurity energy levels caused by chlorine doping, and even the CdTe from the sulfate electrolyte has some energy levels which were attributable to several defects such as Cd or Te vacancies and grain boundaries.²⁹

Electrical properties.— Because the commonly used thickness of CdTe layers employed for a CdTe/CdS solar cell is 1–2 μm , the electrical properties of CdTe in such a thickness range might be of interest in view of the practical applications. The electrical properties of thin CdTe layers (below 3 μm thick), however, could not be determined due to the high resistivity of CdTe. Therefore, the electrical properties need to be measured for thicker layers of approximately 10 μm . In the case of the sulfate and mixed electrolytes, it is relatively easy to prepare such thick layers under illumination because the deposition rates increase due to the photoeffect. Our previous study using sulfate electrolyte revealed that the electrical property of CdTe is not affected by whether or not the layer is prepared under illumination. It is, however, difficult for the chloride electrolyte because the deposition rate is not increased by photoirradiation, as described above. So, a layer with the thickness of 7.5 μm was prepared under illumination for 56 h from the chloride electrolyte and employed to examine the electrical properties. The resistivity, conduction type, carrier density, and carrier mobility are summarized in Table IV. An energy diagram of typical impurity levels formed by the native defects or the chlorine atoms in CdTe^{32–36} is shown in Fig. 8. The conduction type of the chlorine-free CdTe layer obtained from the sulfate electrolyte was p-type, because the majority defect in this layer is Cd vacancy which forms deep acceptor levels at 130 and 210 meV above the top of the valence band.³² Chlorine atoms are known to be substituted for Te atoms in CdTe crystals and form a deep donor level at 350 meV below the bottom of the conduction band.³² In addition, the chlorine atoms form compound defects with native defects such as Cd va-

Table IV. The electrical properties of CdTe layers electrodeposited at potential -0.7 V from three different electrolytes.

	Sulfate electrolyte	Chloride electrolyte	Mixed electrolyte
Resistivity ($\Omega\text{ cm}$)	5.6×10^7	1.1×10^8	1.2×10^8
Conduction type	p	n	p
Carrier density (cm^{-3})	2.1×10^{11}	5.3×10^{10}	1.9×10^{11}
Mobility ($\text{cm}^2\text{ V}^{-1}\text{ s}^{-1}$)	0.54	1.1	0.29
Thickness (μm)	10	7.5	10

cancy or interstitial Te. The compound defect that consists of Cd vacancy and chlorine substituted for Te ($\text{V}_{\text{Cd}}^{2-}/\text{Cl}_{\text{Te}}^{+}$) forms an acceptor level at 120 meV above the top of the valence band.^{33–35} Another compound defect that consists of interstitial Te and chlorine substituted for Te ($\text{Te}_i^{2-}/\text{Cl}_{\text{Te}}^{+}$) also forms an acceptor level, which is located at 60 meV above the top of the valence band.³⁶ Consequently, the chlorine-contaminated CdTe layers obtained from the chloride or mixed electrolyte may be the compensated semiconductors. The layer prepared from the chloride electrolyte showed n-type conduction, probably because the content of chlorine substituted for Te, which forms a donor level, was larger than that of the compound defects which form acceptor levels. In contrast, the layer prepared from the mixed electrolyte still showed the p-type behavior; in this case, the content of chlorine substituted for Te was not enough to develop n-type conduction.

Mobility of the layer prepared from the mixed electrolyte was smaller than that from the sulfate electrolyte, probably due to impurity scattering, which is a phenomenon where the carrier is deprived of kinetic energy by the collision with impure atoms in the crystal. In contrast, mobility of the layer from the chloride electrolyte was the highest of the three because the majority carrier of the layer from the chloride electrolyte is an electron, while that from the others is a hole. Mobility is in inverse proportion to the effective mass of the majority carrier; the effective mass is 0.14 m_0 in the electron and 0.35 m_0 in the hole, where m_0 is the mass of a free electron.³⁷ In contrast, the carrier density reached a low value from 10^{10} to 10^{12} cm^{-3} . This is because relatively deep levels work as trap levels, being formed in the bandgap by the structural defects and the compound defects. Furthermore, it is expected that both mobility and carrier density of the layers with small crystallite grains were reduced because of the scattering and the recombination of carriers in the grain boundaries. In consequence, resistivity of all thin films was about $10^8\text{ }\Omega\text{ cm}$.

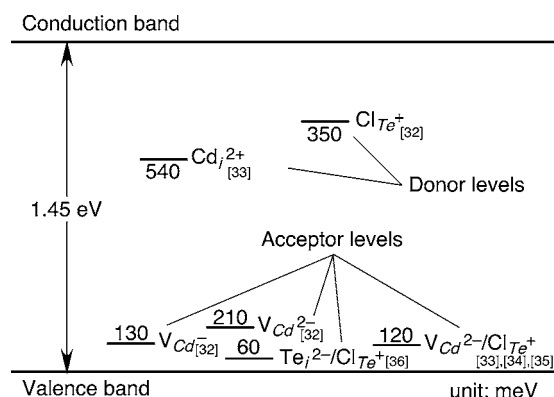


Figure 8. Schematic diagram of donor and acceptor levels formed in the bandgap of CdTe by the native defects and chlorine atoms. References are indicated in brackets.

Conclusion

The paper shows the effect of chloride ions contained in basic ammoniacal electrolytes on CdTe. The increase of current density by irradiating visible light was depressed by chloride ions in the electrolyte, although in the chloride-free electrolyte the current density under illumination was 10–20 times higher than that in the dark. The less noble the cathode potential was and the higher the concentration of chloride ions in the electrolyte was, the more the Cd content of the CdTe films increased. The CdTe deposit from the chloride electrolyte under illumination included a small amount of elemental Cd while the others were almost single-phase polycrystalline CdTe. The CdTe layer electrodeposited from the chloride electrolyte, however, had relatively higher crystallinity both under illumination and in the dark. The bandgap energy of CdTe electrodeposited from the sulfate or chloride electrolyte was evaluated as 1.45 eV, which was almost the same as that of the single-crystal CdTe. The conduction type of the CdTe prepared from the chloride electrolyte was n-type, whereas that of the CdTe from the sulfate or mixed electrolyte was p-type, suggesting that chloride ions involved in the CdTe compound form deep acceptor and relatively shallow donor levels.

Acknowledgments

The authors thank Dr. M. Funato of Kyoto University for his help with the Hall effect measurements. The present work was supported by Grants-in-Aid for Scientific Research (no. 17360370 and 17760593) from the Japan Society for the Promotion of Science (JSPS). The work was also partly supported by General Sekiyu Research and Development Encouragement and Assistance Foundation and by Kyoto University 21st Century COE Program “United Approach to New Materials Science” from the Ministry of Education, Culture, Sports, Science and Technology of Japan.

Kyoto University assisted in meeting the publication costs of this article.

References

1. T. Aramoto, S. Kumazawa, H. Higuchi, T. Arita, S. Shibutani, T. Nishio, J. Nakajima, M. Tsuji, A. Hanafusa, T. Hibino, K. Omura, H. Ohyama, and M. Murozono, *Jpn. J. Appl. Phys., Part 1*, **36**, 6304 (1997).
2. Z. C. Feng, H. C. Chou, A. Rohatgi, G. K. Lim, A. T. S. Wee, and K. L. Tan, *J. Appl. Phys.*, **79**, 2151 (1996).
3. M. A. Hernandez-Fenollosa, D. P. Halliday, K. Durose, M. D. Campo, and J. Beier, *Thin Solid Films*, **431**, 176 (2003).
4. N. Romeo, A. Bosio, V. Canevari, and A. Podesta, *Sol. Energy*, **77**, 795 (2004).
5. C. S. Ferekides, U. Balasubramanian, R. Mamazza, V. Viswanathan, H. Zhao, and D. L. Morel, *Sol. Energy*, **77**, 839 (2004).
6. M. P. R. Panicker, M. Knaster, and F. A. Kröger, *J. Electrochem. Soc.*, **125**, 566 (1978).
7. A. Kampmann, P. Cowache, J. Vedel, and D. Lincot, *J. Electroanal. Chem.*, **387**, 53 (1995).
8. J. L. Stickney, in *Electrochemical Chemistry: A Series of Advances*, A. J. Bard and I. Rubinstein, Editors, Vol. 21, p. 75, Marcel Dekker, New York (1999), and references cited therein.
9. D. W. Cunningham, M. Rubcich, and D. Skinner, *Prog. Photovoltaics*, **10**, 159 (2002).
10. C. Lepiller and D. Lincot, *J. Electrochem. Soc.*, **151**, C348 (2004).
11. J. A. von Windheim and M. Cocivera, *J. Appl. Phys.*, **67**, 4167 (1990).
12. H. Hirato, S. Inamine, K. Nii, and Y. Awakura, *J. Surf. Finish. Soc. Jpn.*, **48**, 728 (1997).
13. K. Murase, T. Hirato, and Y. Awakura, in *Value Addition Metallurgy*, W. D. Cho and H. Y. Sohn, Editors, p. 213, TMS, Warrendale, PA (1998).
14. K. Murase, H. Uchida, T. Hirato, and Y. Awakura, *J. Electrochem. Soc.*, **146**, 531 (1999).
15. K. Murase, I. Nakatani, T. Hirato, and Y. Awakura, *J. Surf. Finish. Soc. Jpn.*, **50**, 367 (1999).
16. K. Murase, H. Watanabe, T. Hirato, and Y. Awakura, *J. Electrochem. Soc.*, **146**, 1798 (1999).
17. K. Murase, H. Watanabe, S. Mori, T. Hirato, and Y. Awakura, *J. Electrochem. Soc.*, **146**, 4477 (1999).
18. K. Murase, M. Matsui, M. Miyake, T. Hirato, and Y. Awakura, *J. Electrochem. Soc.*, **150**, C44 (2003).
19. A. E. Rakhshani, *J. Phys.: Condens. Matter*, **11**, 9115 (1999).
20. G. C. Morris and S. K. Das, *Int. J. Sol. Energy*, **12**, 95 (1992).
21. S. K. Das and G. C. Morris, *J. Appl. Phys.*, **73**, 782 (1993).
22. G. C. Morris, P. G. Tanner, and A. Tottszer, *Mater. Forum*, **15**, 21 (1991).
23. A. Pal, J. Dutta, D. Bhattacharyya, S. Chaudhuri, and A. K. Pal, *Vacuum*, **46**, 147 (1995).
24. M. B. Dergacheva, V. N. Statsyuk, and L. A. Fogel, *J. Electroanal. Chem.*, **579**, 43 (2005).
25. M. Miyake, K. Murase, T. Hirato, and Y. Awakura, *Surf. Coat. Technol.*, **169–170**, 108 (2003).
26. M. Miyake, K. Murase, T. Hirato, and Y. Awakura, *J. Electrochem. Soc.*, **150**, C413 (2003).
27. K. Murase, H. Watanabe, H. Uchida, T. Hirato, and Y. Awakura, *Electrochemistry (Tokyo, Jpn.)*, **67**, 331 (1999).
28. L. J. van der Pawu, *Philips Res. Rep.*, **13**, 1 (1958).
29. K. Arai, K. Murase, T. Hirato, and Y. Awakura, *J. Electrochem. Soc.*, **152**, C237 (2005).
30. File card no. 50674, X-Ray Powder Diffraction Standards, ASTM, Philadelphia, PA.
31. Y. Awakura, K. Murase, and T. Hirato, *High Temp. Mater. Processes (N.Y., NY, U.S.)*, **23**, 383 (2004).
32. Su-Huai Wei and S. B. Zhang, *Phys. Rev. B*, **66**, 155211 (2002).
33. A. E. Rakhshani, *Phys. Status Solidi A*, **169**, 85 (1998).
34. T. A. Kuhn, W. Ossau, A. Waag, R. N. Bicknell-Tassius, and G. Landwehr, *J. Cryst. Growth*, **117**, 660 (1992).
35. S. Seto, A. Tanaka, Y. Masa, and M. Kawashima, *J. Cryst. Growth*, **117**, 271 (1992).
36. V. Valdna, F. Buschmann, and E. Melnikov, *J. Cryst. Growth*, **161**, 164 (1996).
37. A. E. Rakhshani, Y. Makdisi, X. Mathew, and N. R. Mathews, *Phys. Status Solidi A*, **168**, 177 (1998).